

# 3D Building Reconstruction using Stereo Camera and Edge Detection

Konstantinos Bacharidis<sup>1</sup>, Lemonia Ragia<sup>2</sup>, Marios Politis<sup>1</sup>,  
Konstantia Moirogiorgou<sup>1</sup> and Michalis Zervakis<sup>1</sup>

<sup>1</sup>*School of Electronic and Computer Engineering, Technical University of Crete, Kounoupidiana, Chania, Greece*

<sup>2</sup>*School of Environmental Engineering, Technical University of Crete, Kounoupidiana, Chania, Greece*

**Keywords:** Surveying, 3D Building Reconstruction, Stereo Camera Geometry, Image Processing, Edge Detection.

**Abstract:** Three dimensional geo-referenced data for buildings are very important for many applications like cadastre, urban and regional planning, environmental issues, archaeology, architecture, tourism and energy. The acquisition and update of existing databases is time consuming and involves specialized equipment and heavy post processing of the raw data. In this study we propose a system for urban area data based on stereo cameras for the reconstruction of the 3D space and subsequent matching with limited geodetic measurements. The proposed stereo system along with image processing algorithms for edge detection and characteristic point matching in the two cameras allows for the reconstruction of the 3D scene in camera coordinates. The matching with the available geodetic data allows for the mapping of the entire scene on the world coordinates and the reconstruction of real world distance and angle measurements.

## 1 INTRODUCTION

3D spatial data of buildings are very important in recent years for many different applications. In the cadastre and cartography domain, 3D reconstruction of buildings has become a valuable task. For some it is essential to obtain data of mainly handmade objects, such as in environmental management, urban and regional planning, population urbanization, infrastructure, energy, archaeology communication and tourism need the data of cities. More important, managers and city planners must have historical and updated object/building data at the same time.

A very simple method to acquire building data is the computer-aided manual surveying using an electronic distancing meter (Petzold *et al.*, 2004). In this method only distances between two surfaces can be measured. Buildings data have been traditionally acquired with geodetic techniques using the special equipment such as total station. The reflectorless tacheometry is a method based on measuring of geometric dimensions. Although this method is widely used, well established and proved to be accurate, it does have some important disadvantages (Petzold *et al.*, 2004) and every point being measured must be visible from the total station. Laser-scanning is based on measuring distances across every pointing direction to create the point cloud. This method

rapidly captures shapes of buildings with high resolution, but its basic disadvantage is the heavy post-processing of results. Photogrammetry is a well-established method and aerial images have been excessively used for 3D building reconstruction (Gülch *et al.*, 1998) (Fischer *et al.*, 1998). An approach that characterizes a large number of methodologies and techniques for 3D automatic reconstruction of buildings is given by Haala and Kada (Haala and Kada 2010). This study verifies the difficulties to automatically interpret 3D city models to systems without manual intervention. In recent years the detection and reconstruction of 3D geometric model of an urban area with complex buildings is based on aerial LIDAR (Light Detection and Ranging) data (Brenner, 2005) (Elaksher and Bethel, 2002).

In order to deal with inefficiencies of individual modalities of data acquisition, several studies explore the combination of sources. A 3D building reconstruction method that integrates the aerial image analysis with information from large-scale 2D Geographic Information System (GIS) databases and domain knowledge is described by Suveg and Vosselman (Suveg and Vosselman, 2004). The use of aerial images and the exploitation from existing 2D GIS data is also presented (Pasko and Gruber, 1996). The idea for using geodetic techniques combined with

images of uncalibrated camera of historic buildings for restoration in archeology is explored in (Ragia *et al.*, 2015). The idea of using images from Flickr and Picasa to build accurate 3D models for archaeological monuments is presented in (Hadjiprocopis *et al.*, 2014). Especially in the archaeology another approach depicts a 5D multimedia digital model using the 3D model in different time frames (Doulamis *et al.*, 2015). 3D reconstruction from a single image combined with geometrical and topological constraints is further discussed in (Verma *et al.*, 2006).

The method we develop in this paper is towards semi-automatic 3D reconstruction of a building with the geo reference. Although there are a lot of semi-automatic systems for building data acquisition, there are still open problems concerning data gathering, database update and maintain and management of the spatial data. Data sharing and reusing of available spatial information is not always useful because of the alteration or different interpretation of data. In many spatial databases there are inconsistencies about the location of the buildings. Some objects are represented discrete, other appear as lists of individual points on the ground and for some other datasets there is a lack of information about the thematic area.

A list of the main reasons for inadequate or incomplete building data where additional information is needed includes the following.

- Planners who are interested in the traffic system measure only the façade of buildings while the engineers who work for cadastre are interested in acquiring the whole parcels, the buildings and all other objects included in a private parcel like garage and place for sport activities.
- For regional and urban planners the surveying of geometric data plays a dominant role and before modelling or making any decision buildings must be surveyed, in whole or in part of the scene.
- For architectural applications, in many cases the data of the outside of building are available but the architects are interested only in the inside part of the building.
- Maintenance, renovation and change of the usage of a building needs complete 3D reconstruction of a building and sometimes additional geometric information in a bigger scale is required.
- Buildings with extensive alteration need an extensive mapping from many views and for many detailed parts.
- Environmental problems on coastal areas like flooding, dampness and subsidence can create

structural damage of the buildings and new data have to be acquired.

- Different interpretation by the surveyor generate different plans, especially with buildings constructed in an unusual way.
- Restoration of historical building needs an extensive data acquisition of all elements.
- Some errors in the existing data may exist; some measurements may be random.

The proposed approach is an attempt to automatically derive the structural and dimensionality information of a building structure through the matching of its 3D reconstructed coordinates with the real world coordinate system. The building's structural information extracted via image contour estimation techniques provides the points belonging to its skeleton and specifies distance measures that can be specified in actual word dimensions.

The paper is organized as follows. Section 2 describes the stereo layout approach with its characteristics, advantages and limitations for 3D reconstruction of the viewed scene. Moreover, the relation between the 3D metric coordinate system and the 3D physical world system is defined. A discussion on structural information loss due to 3D reconstruction issues along with proposed solutions is presented in Section 3. Finally, the experimental system layout and results are presented in Section 4.

## 2 STEREO LAYOUT AND 3D RECONSTRUCTION

### 2.1 Camera Layout & Coordinate System Relations

The key concept for a successful 3D reconstruction of a scene is the derivation of the scene's depth information. To achieve this target a stereo camera layout can be used, which provides the required relation between the 3D world and 2D coordinate systems allowing the estimation of depth information for the viewing scene.

In order to derive the depth information we need to estimate the parameters expressing the relation between the physical and the image plane systems. Essentially, what we need to estimate is first the relation between the 3D world and the 3D camera systems and then, the mapping parameters between the 3D camera and the 2D image plane coordinate systems. The first set, referred to as extrinsic parameters, consists of the estimation of a Rotation

matrix and a translation vector, whereas the latter, referred to as intrinsic parameters, requires the estimation of the internal camera characteristics such as the focal length. The overall relation between the world and image coordinate systems is expressed as:

$$x = P \cdot X_w \quad (1)$$

with  $x = (x_i, y_i, d, 1)^T$  being the homogenous image coordinates with  $d$  denoting the disparity and  $X_w = (x_w, y_w, z_w, 1)$  being the homogeneous 3D world coordinates of the point  $X_w$ . The operator  $P$  denotes the projection matrix containing the extrinsic and intrinsic parameters describing the relation between the coordinate systems:

$$P = \begin{bmatrix} f & x_o \\ f & y_o \\ 1 & \end{bmatrix} \cdot [R \mid T]$$

where  $[R \mid T]$  is a matrix denoting the extrinsic parameters of the system,  $f$  denoting the camera's focal length and  $(x_o, y_o)$  being the centre coordinates of the recorder picture, defining the intrinsic characteristics.

The stereo layout for each camera and a 3D world point based on eq. (1) defines the following relations for the two (right and left) cameras:

$$x_{left} = P_{left} \cdot X_w \text{ and } x_{right} = P_{right} \cdot X_w \quad (2)$$

All parameters required for the relation derivation can be estimated either by using a camera calibration process (Zhang, 2000) or an uncalibrated approach (Hartley and Zisserman, 2003), (Hartley, 1997), where the projection matrices are estimated through point correspondences. The first approach provides more accurate estimates but is more complicated, whereas the second is simple and exploits known reference points but it may fail in cases whether not significant variations exist between the images of the two cameras.

In the proposed approach we adopt the calibrated methodology, since the appropriate estimation of both intrinsic and extrinsic system parameters lead to more accurate 3D reconstructions. More specifically, these calibrated parameters allow to efficiently reverse distortions introduced during the recording and mapping processes. The calibration is performed through the use of a planar surface, such as a chessboard, which serves as a reference coordinate system. The mapping process aims to assign the camera centers to the reference coordinate system by estimating the rotation and translation that minimizes

the squared distances (Zhang, 2000) between the point correspondences using the direct linear transformation (DLT) algorithm (Bouguet, 2013). The estimation complexity is further increased depending on the stereo layout used, i.e. a non-convergent/parallel layout or a convergent one with the camera pair being rotated at a certain angle (see Fig 1.a, b). The simplest case used at the feasibility study of the proposed method is the parallel stereo layout. In such cases, the common image regions depicted at each image plane are associated through only a translation shift in the x-axis. By performing a matching process, through either the use of simple block matching methods (e.g. (Karathanasis *et al.*, 1996), (Zhang, 2001) or more elaborate ones such as variational approaches (e.g. (Rallim, 2011)), we can estimate this translation map known as disparity map. The disparity refers to the distance between two corresponding points in the left and right image stereo pair (see Fig 1.c):

$$x_{left}(x_i, y_i) = x_{right}(x_i + d, y_i) \quad (3)$$

with  $d$  being the disparity estimate.

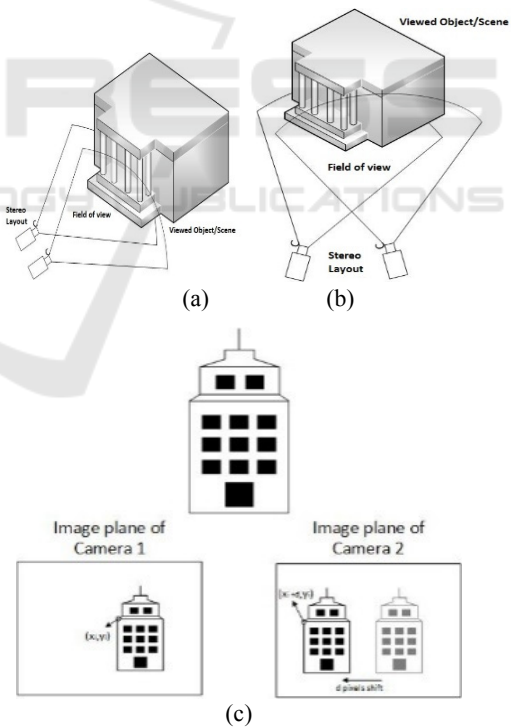


Figure 1: Camera Layouts and image plane relation, (a) Non-convergent/parallel layout, adopted in our approach, (b) convergent layout and (c) the relation between the image planes, each viewed region scene on the left image plane is shifted in the right plane.

## 2.2 3D Reconstruction of the Scene

For each point correspondence  $x_{left} \leftrightarrow x_{right}$  the relation between them and the corresponding 3D world point  $X_w$  is expressed through the relations presented in eq. (2). In order to estimate the depicted world point we must combine the projection matrices and incorporate the restrictions between camera and world points, such as the epipolar constraint. The method of estimating the corresponding 3D world point relating two image plane correspondences is known as triangulation (Hartley and Zisserman, 2003) (see Fig. 2.c). Using the relations presented in eq. (2) and eq. (3) the homogeneous DLT method (4) can be applied leading to a linear system representation of the form  $A \cdot X_w = 0$ , whose solution leads to the estimation of the 3D world point  $X_w$ . The matrix A contains the projection relations between the points and the corresponding world point and is defined as:

$$A = \begin{bmatrix} x \cdot P_{left}^{3T} - P_{left}^{1T} \\ y \cdot P_{left}^{3T} - P_{left}^{2T} \\ x' \cdot P_{right}^{3T} - P_{right}^{1T} \\ y' \cdot P_{right}^{3T} - P_{right}^{2T} \end{bmatrix}$$

with  $P_{left}^i, P_{right}^i$  being the  $i$ -th row vector of the projection matrices  $P_{left}, P_{right}$  for the points

$$x_{left} = (x, y), x_{right} = (x', y')$$

respectively. The vector corresponding to the world point is found through the singular value decomposition (SVD) factorization of the matrix A as  $UDV^T$ , where U and V are orthogonal matrices and D is a diagonal matrix with non-negative entries. The unit singular vector corresponding to the smallest singular value provides the solution for the 3D world point  $X_w$  (Hartley and Zisserman, 2003).

This transformation process allows the estimation of depth information leading to an appropriate reconstruction of the viewing scene. However, the 3D world system does not correspond with the actual 3D world coordinates of the viewing scene. Information about the scene's longitude or latitude cannot be estimated from the stereo layout, e.g. the building's width cannot be estimated. In order to do further knowledge of the viewing scene is required.

For this task we can effectively utilize the geographical coordinates of known points of the building, as derived from the use of specialized geo-

reference systems, such as GPS, in combination with the coordinates estimated from image processing, as to estimate the missing information. For example, in the derivation of a building's contour, we could use the adjacent point relation in world coordinates in the form of width or height, to estimate the missing dimensions of the building. Besides this use, available points with their world coordinates can be used as validation for the depth estimation accuracy or as a means of refining the depth estimate during the depth estimation process.

## 2.3 Combining Geo-referencing with 3D Reconstruction

We mentioned earlier that the 3D reconstructed building can be associated with geo-referenced points to allow the derivation of the missing dimensionality information of the structure. This task is essentially a new mapping process between the estimated metric 3D coordinate system and the 3D physical world coordinate system. The transformation relation between these systems is of the form:

$$X_{Gw} = \lambda R \cdot X_w + T \quad (4)$$

with  $X_{Gw} = (x_{Gw}, y_{Gw}, z_{Gw})^T$  is the 3D world geo-referenced ground point,  $X_w = (x_w, y_w, z_w)^T$  is the 3D metric world coordinate system,  $\lambda$  is the transformation parameter and R, T are the rotation matrix and translation vector required to relate the coordinate systems.

Given points with known geo-reference coordinates (at least 8 points), we can estimate the transformation parameters ( $\lambda, R, T$ ) using a least-squares minimization scheme. The estimated transformation parameters enable to relate every 3D metric on the reconstructed points to the corresponding physical world 3D coordinates.

We can use these transformations to estimate the 3D physical coordinates of the building, or to compute its structural dimensionality information (width, height, volume). To speed up the estimation process we isolate the buildings morphological structure through image processing by extracting its contour. We can then estimate the 3D physical coordinates of the points belonging to the building's contour and thus, acquiring all the information needed for estimating the building's real world structural morphology. In the following section we present the method utilized for the extraction of the building's contour information using image processing.

Expanding the geo-referenced points' (GPs) role in the stereo rig, we can skip the utilization of a reference system in the calibration process (chessboard pattern). Instead, if an appropriate number of GPs is known satisfying the requirements that a) the corresponding points are visible on the camera planes and b) the geo-referencing is accurate, then we can set the world coordinate system defined by these points as our reference system. Towards this direction we need to employ a point identification method for locating these points in the camera images and then use these correspondences to perform the calibration of the stereo rig.

## 2.4 3D Reconstruction Ambiguity and Limitations

The use of a parallel stereo layout, although simplifying the depth estimation process, provides partial reconstruction for the structure, i.e. only for the single view of the structure facing the stereo layout. To produce a more complete 3D reconstruction of the entire building, we can initially use a convergent stereo layout with the cameras being rotated at a certain angle, thus increasing the viewing angle of the building's structure being recorded. The second, more effective approach is to combine different viewing positions of the stereo layout, map them to the same reference system and stitch together all 3D reconstructions of the building sides to form a single 3D representation.

If we now consider the case where we use a convergent layout with the cameras displaying the viewing object at different angles the reconstruction accuracy depends on a) whether a calibrated approach is used or not and b) how the additional distortions introduced by the layout formation, such as the keystone distortion, affects the estimation accuracy. Similar to the parallel stereo rig layout a calibrated approach will produce more accurate estimates taking advantage of the impact of the distortions introduced, allowing for some cases to undo their affect, however requiring more complicated estimation processes. An uncalibrated convergent stereo rig, although simpler, will be prone to projective ambiguity in the reconstruction process. This is due to the fact that in the uncalibrated approach the only assumption made is that all rays back-projecting from the reconstructed 3D point must intersect the image plane leading to dimensionality deformations in the reconstructed object. The projective reconstruction reflects intersection and tangency, however it fails to preserve the angles, the relative lengths and the volume of the 3D reconstructed object. This projective

reconstruction loss does not happen in the calibrated approach, since the estimation of the relation between camera and world coordinate systems, as well as the epipolar constraint relations, do not alter or deform the viewing angle between the rays. This enables preservation of the parallelism, volume, length ratio as well as of the angles of the reconstructed object, leading to a similarity reconstruction.

The reconstruction of an uncalibrated approach can be further strengthened leading to an affine reconstruction that preserves the volume ratios and the parallelism of the object. Towards this direction we can use scene constraints and conditions, such line parallelism indicating vanishing points, which allow the estimation of a the epipolar plane lying at infinity passing through the two camera centers.

Closing this topic, the selection of a calibrated approach, such as the one deployed in our proposal, although requiring more complex transformation systems, will lead to a more detailed reconstruction for the viewed object/building, preserving the structural and volumetric characteristics.

## 3 LINE SEGMENTS EXTRACTION

The previous section has described the methodology for derivation of the 3D scene information. Since the aim of the proposed method is to extract the 3D morphological characteristics and dimensionality information of the building present in the viewing scene, we need to isolate the building from the entire scene and extract its contour and other linear structures, so that a relation between the estimated 3D physical coordinates of the scene and the building's estimated structure can be derived.

This section addresses techniques to locate and measure straight line segments belonging to a building's main structure. The main idea is to locate several straight line segments that exist in the image edge map. It is noted that this process mainly focuses on the extraction of line segments that lie on the building's main structure (along its horizontal width and vertical height), while more complex and detailed objects (such as bars, rails, small windows and signs, etc.) are not taken into account in our implementation. The basic steps of the algorithm are outlined below, with a further explanation on the utility of each step.

- Image color segmentation through K-Means.
- Automatic image Thresholding and conversion to binary image.
- Edge Detection

- Edge Linking
- Straight line fitting using the Hough Transform

### 3.1 Image Color Segmentation

Given the RGB image of the target building, we firstly convert it to the corresponding HSV (Hue-Value-Saturation) model and then extract only the Hue and Value channels prior to applying our Segmentation scheme. The method used for the color segmentation is the K-Means Clustering (Lloyd, 1982). This iterative method is employed to partition all of the image's pixels  $p = [p_1, p_2 \dots p_n]$  into  $k$  clusters  $C = [C_1, C_2 \dots C_k]$ , where obviously  $k \leq n$ . The clustering is achieved through the minimization of the following value:

$$\arg \min_C \sum_{i=1}^k \sum_{p \in C_i} \|p - \mu_i\|^2 \quad (5)$$

where  $\mu_i$  is the mean of the points that belong to  $C_i$ .

As the equation above states, the K-Means clustering method firstly calculates each pixel's Euclidean distance from the mean value of the cluster it belongs to. This mean value is often called the cluster center or the cluster centroid value. Then it proceeds with calculating the sum of these distances for each cluster separately and minimizing the total distance metric for each cluster. The minimization procedure runs iteratively (MacKay, 2003).

At the first iteration,  $k$  random pixels are assigned as cluster means,  $\mu^{(t=0)} = [\mu_1, \mu_2, \dots, \mu_k]$ , thus creating the initial clusters. Then, the squared distance of each pixel from all the mean values is computed and each pixel is enlisted to the cluster whose mean value is the nearest. In the next step, the new mean values are estimated from the current clusters through the equation:

$$\mu_i^{(t+1)} = \frac{1}{|C_i^{(t)}|} \sum_{p_j \in C_i^{(t)}} p_j$$

The whole process terminates when the classification of the pixels to new clusters no longer changes.

When the method is terminated, each pixel will have obtained a label corresponding to the cluster that has been assigned to. In this way we can segment the image into several color-dependent clusters. In our algorithm, we choose  $k=7$  (number of distinctive colors in the image) and repeat the whole process three times to avoid local minima. The building's pixels will have acquired the same integer value(label) by the segmentation technique and by setting to 0 all the pixels' values in the initial image

that have obtained a different label we efficiently isolate the building. Thus, the color difference of the building from the rest of the image's objects is modeled through difference in intensity of the cluster representing the building and the rest of the clusters. The initial RGB image as well as the image with the isolated building are depicted in the figure below (see Fig. 2).



(a)



(b)

Figure 2: Image color segmentation using k-means method. (a) A picture of a building in Technical University of Crete in its original RGB form. (b) The image of the cluster containing the building, after the k-means method has been applied, having isolated up to a degree the building from other objects like vegetation, the sky etc.

### 3.2 Image Thresholding

In order to compute a global threshold to convert the building-cluster image to a binary image, Otsu's technique is used (Otsu, 1979). This method is based on the idea that the pixels of the image are initially divided into various intensity levels and tries to classify the pixels into only two regions (black and white) as efficiently as possible with a single global threshold. In other words, Otsu's method criterion is the maximization of the distinctiveness between "light" and "dark" areas in the image. Assuming an initial threshold value the pixels are divided into two classes. The possibilities for a pixel  $p$  to belong to one of the two classes are  $\omega_1(\kappa)$  and  $\omega_2(\kappa)$  and they depend on the chosen threshold value  $\kappa$ , as different  $\kappa$  values will result in different pairs of classes. For  $L$  initial intensity levels the following equations apply:

$$\omega_1(\kappa) + \omega_2(\kappa) = 1 \quad (6)$$

$$\omega_1(\kappa)\mu_1(\kappa) + \omega_2(\kappa)\mu_2(\kappa) = \mu_L \quad (7)$$

where  $\mu_L$  is the total mean value over all of the  $L$  intensity values and  $\mu_1, \mu_2$  are the mean values of the two classes. Moreover:

$$\sigma_w^2(\kappa) = \omega_1(\kappa)\sigma_1^2(\kappa) + \omega_2(\kappa)\sigma_2^2(\kappa) \quad (8)$$

$$\sigma_L^2 = \sigma_w^2(\kappa) + \sigma_\beta^2(\kappa) \quad (9)$$

The factor  $\sigma_w(\kappa)$  is the intra-class standard deviation whereas the term  $\sigma_L$  is the total standard deviation for the whole image without a threshold. As Otsu has proved:

$$\begin{aligned} \sigma_\beta^2(\kappa) &= \sigma_L^2 - \sigma_w^2(\kappa) \\ &= \omega_1(\kappa)\omega_2(\kappa)[\mu_1(\kappa) - \mu_2(\kappa)]^2 \end{aligned} \quad (10)$$

so that minimizing the intra-class standard deviation is equivalent to maximizing  $\sigma_\beta$ , as  $\sigma_L$  remains constant.

Specifically, for all the possible threshold values  $\kappa_i$  the algorithm computes the  $\sigma_\beta^2(\kappa_i)$  values according to eq.(10). The optimum threshold value  $\kappa_T$  corresponds to the minimum of all the different  $\sigma_\beta^2(\kappa_i)$  values. Once the threshold has been computed, we are able to effectively convert our intensity image to a binary image.

As a last step of this stage, we remove from the binary image all connected components that have fewer than 5000 pixels by means of area opening, in order to further isolate the building from various “noisy” structures.

### 3.3 Edge Detection

In our implementation, the Canny method is used for edge detection. This method is effective against noise and is likely to detect weak edges. Its effectiveness lies on the fact that it uses two thresholds, a low

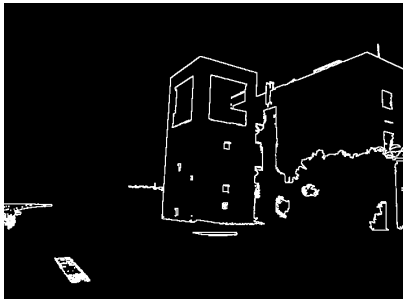


Figure 3: Binary edge image after Canny edge detector is applied. For viewing purposes, the edges have dilated using a 9x9 block of 1s.

threshold to detect strong edges and a high threshold for weak edges. The weak edges are included in the output image only if they are connected to strong edges. The low and high threshold values selected in this algorithm are 0.022 and 0.126 respectively. Moreover, the standard deviation  $\sigma$  of the Gaussian filter applied by the Canny detector is 1.65. The resulting edge map is depicted in Fig. 3.

### 3.4 Edge Linking

A common step after the binary edge image has been computed is edge linking. The objective is to fill gaps that might exist between edge segments and link edge pixels into straight edges. The implementation is based on the idea of indirectly connecting the endpoints of two close edge segments by placing a certain structuring element in between those points. The structure used is a small disk. If the endpoints of two edge segments are close enough to each other, then the two disks placed at each one will overlap. Then an image thinning follows, resulting in a line at the overlapping point and thus linking the two previously unlinked endpoints. In addition, if there is no other endpoint near enough, the thinning will result in the disk's erosion. In our implementation, the radius of the disk is 3 pixels.

To locate endpoints of edges we set up a lookup table by passing all possible 3 x 3 neighborhoods to a certain function, one at a time. This function tests whether the center pixel of the neighborhood is an endpoint. In order for this to happen, the center pixel must be 1 and the number of transitions between 0 and 1 along the neighborhood's perimeter must be two.

#### Line Modelling with Hough Transform:

In order to locate straight line segments on a binary image or an edge map, the Hough Transform technique is employed. It is a powerful method that finds shapes whose curve is expressed by an analytic function, for instance, a line. A line is expressed by the equation:

$$y = mx + c \quad (11)$$

However, because the  $m$  value of vertical lines is infinity, a more convenient and computationally reasonable approach is used (Duda and Hart, 1972).

Thus, the line is expressed in polar coordinates as:

$$\rho = x\cos\theta + y\sin\theta \quad (12)$$

where  $\rho$  is the distance from the origin of the plane to the line and  $\theta$  is the angle between the horizontal  $x$ -

axis and  $\rho$ . Following this approach, a line in the  $(x, y)$  plane corresponds to a single point in the  $(\theta, \rho)$  plane.

In our implementation, we extract peaks with integer values greater than the ceiling integer of the 30% of the maximum value of the accumulator matrix. The lines illustrated in Figure 4 have  $\theta$  values in the ranges  $[-2^\circ, 5^\circ]$ ,  $[175^\circ, 185^\circ]$ ,  $[-70^\circ, -85^\circ]$ ,  $[50^\circ, 55^\circ]$  and  $[65^\circ, 70^\circ]$ . It is noted that some of the lines illustrated are produced by merging smaller line segments associated with the same Hough transform bin. Merged lines shorter than 150 pixels are discarded.



Figure 4: Lines belonging to the main structure of the target building and detected using the Hough transform. The yellow and red asterisks correspond to a line's beginning and end points respectively.

#### 4 RESULTS AND EXPERIMENTAL SET-UP

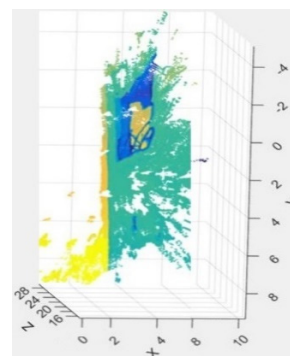
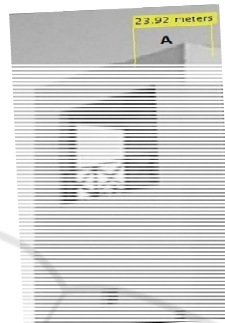
The proposed system consists of a stereo rig of CCD Cameras, in a non-convergent/parallel layout formation (see Fig 1. a) with baseline distance of 5.6 cm, simulating the human visual system layout. The intrinsic and extrinsic parameters of the system are computed through the multi-view calibration process described above. The triangulation procedure described in section 2.2 allows the 3D reconstruction of the building, as illustrated in Fig 5.b.

In our case of study, three GP points on the building's rooftop (marked blue in Fig 5.a) with known geo-referenced physical coordinates are initially used for evaluating the physical dimensions of depth estimates. Notice that with the addition of 8 more GPs and by solving the linear equation system defined by the relations described in eq. (3) we end up with the transformation parameters relating the 3D real world coordinate system with the 3D metric based reconstructed building system.

We can observe from figure 5 that the depth map can be efficiently reconstructed, as long as we have



(a)



(b)

Figure 5: (a) The viewed scene with blue points indicating those with known Geo-referenced coordinates used as validation for the derived depth map and the corresponding depth estimates (yellow boxes) based on the 3D metric coordinates, (b) A 3D reconstruction of the left side of the building using the triangulation approach. Different colours indicate homogeneous regions at different depth.

many corner points available. As far as length estimation between pairs of points of scene is concerned, we consider the two circled corner points of Figure 5 (a). The calibrated stereo layout leads to a deviation error of 0.73  $(5.38 - 4.65)$  m or 13.57%. We have used the known Geo-reference coordinates of the building's edges (blue points in Fig.5a) as a validation for the depth estimates. The calculated depth difference between points A and B based on our depth estimates marked with yellow boxes in Fig 6.a is 3.65m whereas, the corresponding difference based on their Geo-reference coordinates is 5.38m. The depth deviation can be further reduced with the addition of pre-processing and post-processing steps prior and posterior the depth derivation process. Illumination invariance and image enhancement prior the camera calibration stage can improve the estimation of the stereo layout characteristics and relations by removing shadowing and uneven illumination or noise effects, leading eventually to better depth estimates. As a post-processing

measure, we can incorporate scene constraints and conditions. For example, 3D line parallelism and point intersection conditions or ground truth point employment can serve as constraints and homography estimation boundaries, reducing the reconstruction ambiguity (Hartley and Zisserman, 2003).

Following the proposed procedure, we extract the building structure through the use of edge detection, contour extraction and line structure estimation methodology (see Fig. 6.a). We can now isolate the points belonging to the building structure and contour (see Fig 6.b, red box). Finally, by associating the points belonging to the building's contour with their 3D world coordinates, we can derive all necessary information required to estimate the building's real world dimensionality (width, height and length). In addition, using the Geo-referencing system we can Geo-reference the building's whole structure, its location and volume in the real world physical system.

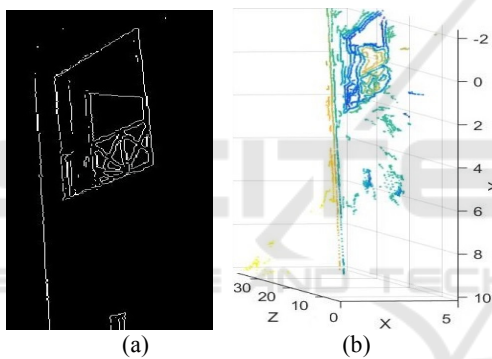


Figure 6: (a) Isolated structure of the building (red box) using line segment method and (b) isolated 3D reconstruction of the points belonging to the structure.

## 5 CONCLUSIONS

We propose an approach for automatic extraction the structural and geometrical information of buildings. The ultimate task is to provide the entire scene and its buildings in a georeferenced form and achieve a correspondence of its feature measurements with the real world. The proposed approach exploits a stereo camera system in association with appropriate image processing tools, which enable an initial reconstruction of the scene mapped on the camera coordinates. Subsequently, we use a limited number of geodetic measurements as reference in order to map the scene onto world coordinates. An important issue in our methodology is the successful 3D

reconstruction and the estimation of depth. Our future aim is to further improve our estimation with the application of pre-processing and post-processing methodologies that will reduce both the scene and estimation dependent deviation effects that lead to reconstruction ambiguities. The isolation of specific building structures from the scene can facilitate this estimation process. Overall, it is demonstrated that the use of stereo camera enables the relation between the 3D georeferenced system and the camera coordinated system, so that depth information can be extracted.

## REFERENCES

- Doulamis, A., Doulamis, N., Ioannidis, C., Chrysouli, C., Grammalidis, N., Dimitropoulos, K., Potsiou, C., Stathopoulou, E., K., Ioannides, M., 2015. 5D Modelling: An Efficient Approach for Creating Spatiotemporal Predictive 3D Maps of Large-Scale Cultural Resources. *ISPRS Annals of Photogrammetry, Remote Sensing and Spatial Information Sciences*, 1, pp. 61-68.
- Hadjiprocopis A., Ioannides, M., Wenzel, K., Rothermel, M., Johnsons, P., S., Fritsch, D., Doulamis, A., Protopapadakis, E., Kyriakaki, G., Makantasis, K., Weinlinger, G., Klein, M., Fellner, D., Stork, A., Santos, P., 2014. 4D reconstruction of the past: the image retrieval and 3D model construction pipeline. In *Second International Conference on Remote Sensing and Geoinformation of the Environment (RSCy2014)* International Society for Optics and Photonics, pp. 922916-922916.
- Moore, R., Lopes, J., 1999. Paper templates. In *TEMPLATE'06, 1st International Conference on Template Production*. SCITEPRESS.
- Smith, J., 1998. *The book*, The publishing company. London, 2<sup>nd</sup> edition.
- Petzold, F., Bartels, H., Donath, D., 2004. New techniques in building surveying. *Proceedings of the ICCCB-X*, pp 156.
- Gülch, E., Müller, H., Labe, T. and Ragia, L., 1998. On the performance of semi-automatic building extraction. *International Archives of Photogrammetry and Remote Sensing*, 32, pp. 331-338.
- Fischer, A., Kolbe, T. H., Lang, F., Cremers, A. B., Förstner, W., Plümer, L. and Steinhage, V., 1998. Extracting buildings from aerial images using hierarchical aggregation in 2D and 3D. *Computer Vision and Image Understanding*, 72(2), pp. 185-203.
- Haala, N., Kada, M., 2010. An update on automatic 3D building reconstruction. *ISPRS Journal of Photogrammetry and Remote Sensing*, 65(6), pp. 570-580.
- Suveg, I., and Vosselman, G., 2004. Reconstruction of 3D building models from aerial images and maps. *ISPRS*

- Journal of Photogrammetry and remote sensing*, 58(3), pp. 202-224.
- Pasko, M. Gruber, M., 1996. Fusion of 2D GIS Data and aerial images for 3D building reconstruction. *International Archives of Photogrammetry and Remote Sensing*, vol. XXXI, Part B3, pp. 257-260.
- Ragia, L., Sarri, F., Mania, K., 2015. 3D Reconstruction and Visualization of Alternatives for Restoration of Historic Buildings – A new Approach. Proceedings of the 1<sup>st</sup> International Conference on Geographical Information Systems Theory, Applications and Management, Barcelona, Spain, 28-30 April, pp. 94-102.
- Brenner, C., 2005. Building reconstruction from images and laser scanning. *International Journal of Applied Earth Observation and Geoinformation*, 6(3), pp. 187-198.
- Verma, V., Kumar, R. and Hsu, S., 2006. 3D building detection and modeling from aerial LIDAR data. In *Computer Vision and Pattern Recognition, IEEE Computer Society Conference on* Vol. 2, pp. 2213-2220.
- Elaksher, A. F., and Bethel, J. S., 2002. Reconstructing 3D buildings from LIDAR data. *International Archives Of Photogrammetry Remote Sensing and Spatial Information Sciences*, 34(3/A), pp. 102-107.
- Zhang, Z., 2000. A flexible new technique for camera calibration. *IEEE Transactions on Pattern Analysis and Machine Intelligence*. vol. 22(11), pp. 1330-1334.
- Hartley, R., Zisserman, A., 2003. *Multiple View Geometry in Computer Vision*. Cambridge University Press.
- Hartley, R., 1997. In Defense of the Eight-Point Algorithm. *IEEE Transactions on Pattern Analysis and Machine Intelligence*, v.19 n.6.
- Bouguet, J., 2013. Camera calibration toolbox for MATLAB. [http://www.vision.caltech.edu/bouguetj/calib\\_doc/](http://www.vision.caltech.edu/bouguetj/calib_doc/)
- Karathanasis, J., D. Kalivas, D., and J. Vlontzos, J., 1996. Disparity estimation using block matching and dynamic programming. *IEEE Conference Electronics, Circuits and Systems*, pp.728 -731.
- Zhang, L., 2001. Hierarchical block-based disparity estimation using mean absolute difference and dynamic programming. Proceedings International Workshop Very Low Bit-Rate Video Coding (VLBV01), pp.114 -117.
- Rallim, J., 2011. PhD thesis, Fusion and regularization of image information in variational correspondence methods, Universidad de Granada. Departamento de Arquitectura y Tecnología de Computadores, <http://hera.ugr.es/tesisugr/20702371.pdf>
- Lloyd, S. P. (1957). "Least square quantization in PCM". Bell Telephone Laboratories Paper.
- Lloyd, S. P. (1982). "Least squares quantization in PCM", *IEEE Transactions on Information Theory* 28 (2): 129–137.
- MacKay, David (2003). "Chapter 20. An Example Inference Task: Clustering" *Information Theory, Inference and Learning Algorithms*. Cambridge University Press. pp. 284–292.
- Nobuyuki Otsu (1979). "A threshold selection method from gray-level histograms". *IEEE Trans. Sys., Man., Cyber.* 9 (1): 62–66.
- Duda, R. O. and P. E. Hart, "Use of the Hough Transformation to Detect Lines and Curves in Pictures," *Comm. ACM*, Vol. 15, pp. 11–15 (January, 1972)